

# The Ag I and Au I Resonance Line Broadening in Helium Plasma

Stevan Djeniže<sup>a</sup>, Aleksandar Srećković<sup>a</sup>, Srdjan Bukvić<sup>a</sup>, and Nikola Vitas<sup>b</sup>

<sup>a</sup> Faculty of Physics, University of Belgrade, Studentski trg 16, 11 001  
Belgrade, P. O. Box 368, Serbia

<sup>b</sup> Department of Astronomy, Faculty of Mathematics, University of Belgrade,  
Studentski trg 14, 11 001 Belgrade, Serbia

Reprint requests to Prof. S. D.; E-mail: steva@ff.bg.ac.yu

Z. Naturforsch. **61a**, 491 – 498 (2006); received May 25, 2006

The shapes and shifts of the resonance spectral lines of neutral silver (Ag I: 328.068 and 338.289 nm) and gold (Au I: 242.795 and 267.595 nm) have been measured in a laboratory helium plasma of about 18,500 K electron temperature and an electron density ranging between  $0.78 \cdot 10^{23}$  and  $1.24 \cdot 10^{23} \text{ m}^{-3}$ . Stark broadening has been found as the dominant mechanism of the line shape and position formation. Our measured Ag I and Au I resonance line Stark widths ( $W$ ) and shifts ( $d$ ) are the first reliable experimental data. They are compared with calculated single Ag I and Au I  $W$  and  $d$  data based on a semiclassical approach. The measured values are higher than the calculated ones, especially of the Au I resonance lines. Besides, we have calculated the hyperfine structure (hfs) components and their relative intensities of the mentioned Ag I and Au I lines. Strong asymmetry between the red and blue components of the hfs was found. A modified version of the linear, low-pressure, pulsed arc was used as plasma source operated in helium with silver and gold atoms as impurities, evaporated from silver and gold cylindrical plates located in the homogeneous part of the discharge providing conditions free of self-absorption. At the above mentioned helium plasma conditions the splitting in the hyperfine structure ( $\Delta_{\text{hfs}}$ ) of the Ag I and Au I resonance lines has been overpowered by Stark and Doppler broadenings. We estimate that at electron densities below  $10^{20} \text{ m}^{-3}$  and electron temperatures below 10,000 K the hfs components in the 267.595 nm and 242.795 nm Au I lines play an important role in the line shape formation, and the resulting line profiles can be used for temperature estimation in optically thin plasmas.

*Key words:* Plasma Spectroscopy; Line Profiles; Atomic Data.

## 1. Introduction

Several works deal with the presence of gold and silver in cosmic spectra [1 – 3]. Silver and gold atoms are also present in many chemical and physical processes [4, 5]. Thus, the spectral lines of neutral silver (Ag I) and gold (Au I) can play an important role in plasma diagnostics. Among them, the intense resonance lines are the most useful. Their shape characteristics (line width and line center position) can be used for plasma diagnostics and modeling [6, 7]. These characteristics are determined by interactions within the atom (within electrons in core + core-nucleus interaction), by interactions between atoms and external fields (Stark and Zeeman effects) and by the thermal motion causing the Doppler effect [7]. The resulting line shape reflects also the self-absorption. Combination of various plasma conditions, expressed through plasma parameters like: electron density ( $N$ ), electron temperature

( $T$ ), magnetic field strength ( $B$ ), species densities, are responsible for the line shape and line center position. An always recognizable contribution to the line shape comes from the emitter itself, due to possible splitting ( $\Delta_{\text{hfs}}$ ) in the hyperfine structure (hfs). The hyperfine structure of the spectral line is caused by the interaction of the electron angular momentum ( $J$ ) with the nuclear spin ( $I$ ). The splitting of the spectral line depends on the nuclear magnetic dipole moment and the electric quadrupole moment [8], and can be ranged in a wide wavelength interval. Besides, the isotope effect can influence the distribution of the components in the  $\Delta_{\text{hfs}}$ . Silver and gold have the nuclear spin  $I = 1/2$  and  $I = 3/2$ , respectively [9]. One can expect higher hfs splitting in the Au spectral lines independent of the isotope effect. Namely, only one gold isotope ( $^{197}\text{Au}$ ) exists in the natural stage. Silver has two stable isotopes (51.84%  $^{107}\text{Ag}$  and 48.16%  $^{109}\text{Ag}$ ). The hfs splittings in the resonance Ag I lines were measured by Hill [10].

They are small, about 0.6 pm. For the Au I resonance lines Ritschl [11] and Elliott and Wulff [12] have found  $\Delta_{\text{hfs}} = 1.58$  pm (approximately), which is about 2.5 times higher than those of the resonance Ag I lines. The experimentally found number of hfs components in the resonance Ag I and Au I spectral lines was two. In cold plasmas with small  $B$  and  $N$  values the hfs components give the most significant contribution in the line shape formation.

In plasmas with  $N$  higher than  $10^{21} \text{ m}^{-3}$  the Stark broadening begins to play an important role in the spectral line shape and line center position [7]. Thus, the Stark broadening parameters (the width  $W$  and the shift  $d$ ) may be useful in the modeling and diagnostics of various plasmas. However, no reliable experimental  $W$  and  $d$  values of the Ag I and Au I resonance spectral lines exist (see [13] and references therein). Only two works are dedicated to the calculation of the Ag I [14] and Au I [15]  $W$  and  $d$  parameters. In both the semiclassical approach was applied.

The aim of this work is to present the first reliable measured Ag I and Au I resonance lines Stark FWHM (full-width at half of the maximal intensity,  $W$ ) and  $d$  parameters. They are compared with the splitting ( $\Delta_{\text{hfs}}$ ) in the hyperfine structure (calculated by us and other authors) and with the Doppler width ( $W_{\text{D}}$ ), depending on the temperature. In order to ensure homogenous distribution of the silver and gold atoms in the helium plasma, a new discharge tube has been constructed.

## 2. Experimental

A modified version of the linear, low-pressure arc [16, 17] has been used as plasma source. A pulsed discharge was created in a Pyrex discharge tube of 5 mm inner diameter and plasma lengths of 12 and 14 cm. The tube had an end-on quartz window. In order to provide a uniform distribution of the silver and gold atoms in the monitored part of the plasma, thin silver (200  $\mu\text{m}$ ) and gold (150  $\mu\text{m}$ ) cylindrical plates (99.9% purity) have been posted inside the cylindrical part (see Fig. 1 in [16]) of the discharge tube on its ends. The length of plates was 16 mm and 23 mm for Ag and Au, respectively. The position of the plates provide a uniform distribution of the evaporated Ag and Au atoms along the optical axis of the homogeneous part of the discharge, while the density of the evaporated silver and gold atoms remained low and the plasma can be considered as optically thin for the investigated lines.

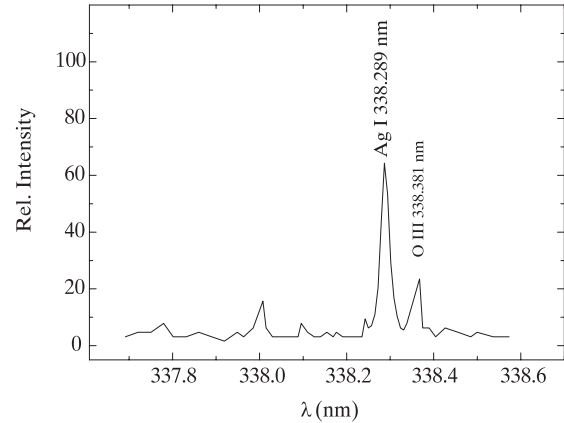


Fig. 1. The 338.289 nm Ag I line profile recorded by the step-by-step technique (seven shots at the same position).

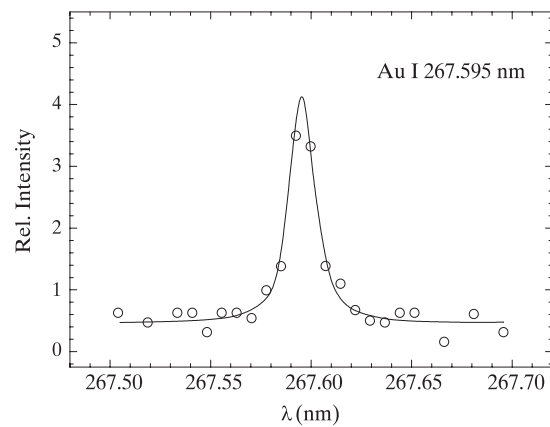


Fig. 2. The 267.595 nm Au I line profile recorded by the step-by-step (7.3 pm) technique (seven shots at the same position). Circles represent measured values. The solid line represents the corresponding Voigt profile using 0.0049 for the Gaussian parameter ( $\beta_2$ ) in the fitting procedure. The baseline is determined using the procedure described in [23].

The absence of self-absorption was checked, using the method described in [18]. Concerning this method, we have monitored ratios of relative line intensities. The relative intensity ratios of the resonance Ag I lines to the 546.550 nm Ag I line and the resonance Au I lines to the 627.817 nm Au I line remained constant during the plasma decay from the 25<sup>th</sup>  $\mu\text{s}$  after the beginning of the discharge. The line profiles were analyzed after the 30<sup>th</sup>  $\mu\text{s}$  in the decaying plasma. The working gas was helium (90% He + 7% N<sub>2</sub> + 3% O<sub>2</sub>) flowing at 665 Pa with Ag and Au plates, respectively. A capacitor of 14  $\mu\text{F}$  was charged up to 63 and 34 J bank energy, respectively. The plasma reproducibility was controlled by monitoring the radiation originating from the

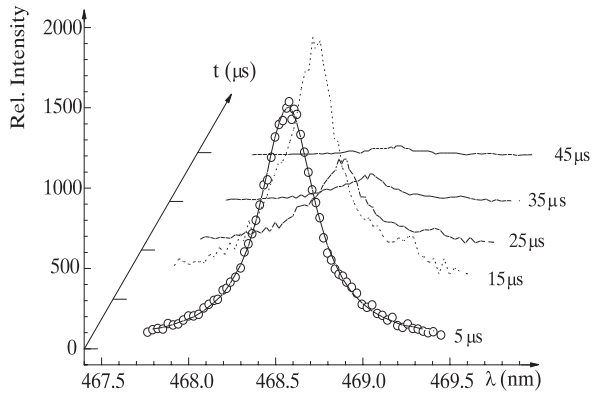


Fig. 3. Temporal evolution of the  $P_\alpha$  (468.6 nm) He II spectral line profile used for the electron density ( $N$ ) determination during the plasma decay (case of the He + Au plasma). Circles represent measured values at 5  $\mu\text{s}$  after the beginning of the discharge. Solid line at 5  $\mu\text{s}$  represents the corresponding Lorentz profile with  $(0.40 \pm 0.02)$  nm FWHM (full-width at half of the maximal intensity).

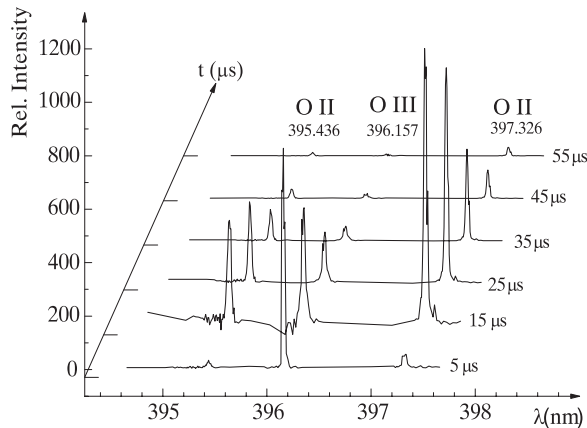


Fig. 4. Temporal evolution of the O II and O III spectral line intensities used for the electron temperature ( $T$ ) determination during the plasma decay (case of the He + Au plasma).

He I, He II, O II and O III lines and the discharge current, using a Rogowski coil signal (it was found to be within  $\pm 4\%$ ). The spectroscopic observations of spectral lines were made end-on along the axis of the discharge tube. The line profiles were recorded using a step-by-step (7.3 pm) technique with the experimental set-up system described in [19–22]. This technique enables monitoring the line shapes continually during the plasma decay and gives the possibility to compare line shapes mutually among various stages of the same plasma. The photomultiplier signal was digitized using a digital scope interfaced to a computer. At each wavelength step, seven shots have been recorded and sub-

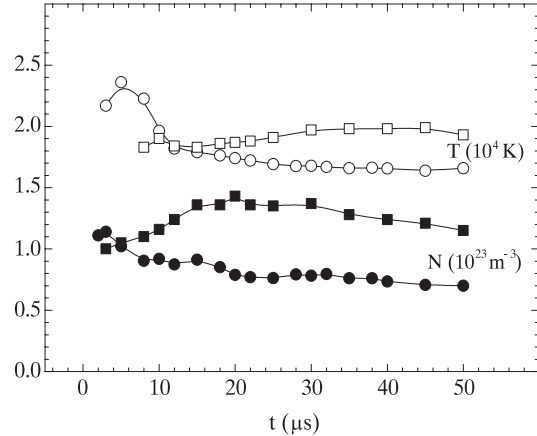


Fig. 5. Temporal evolution of  $T$  and  $N$  values during the plasma decay. The symbols  $\square$  and  $\blacksquare$  are related to the  $T$  and  $N$  values, respectively, in the case of the He + Ag plasma, while  $\circ$  and  $\bullet$  describe mentioned plasma parameters in the case of the He + Au plasma.

sequently averaged. Some of the recorded line profiles are given in Figs. 1 and 2.

The plasma parameters were determined using standard diagnostic methods. Thus, the electron density decay was determined using the known Stark FWHM of the He II  $P_\alpha$  (468.6 nm) spectral line [7] within  $\pm 9\%$  accuracy. Temporal evolution of the  $P_\alpha$  line profile is presented in Figure 3. The electron temperature was obtained using the relative intensity ratio method (Saha equation in [6]) between the O II (395.436 nm and 397.326 nm) and O III (396.157 nm) spectral lines with an estimated error of  $\pm 13\%$ , assuming the existence of local thermodynamical equilibrium (LTE). The necessary atomic data are taken from [13]. The temporal evolution of the O II and O III line intensities is presented in Figure 4. Temporal evolutions of the electron density  $N$  and the electron temperature  $T$  are presented in Figure 5.

### 3. Line Width and Shift Measurements

In existing works, dedicated to the splitting in the hyperfine structure of Ag I and Au I, the emitters are essentially cold and free of intensive electric fields. On the other hand, our light source is a high temperature (about 18,500 K) high electron density ( $10^{23} \text{ m}^{-3}$ ) plasma. Consequently, one can expect a complex behavior caused by high temperature and high electron density. The effect of the high temperature will be examined first, i. e., other broadening mechanisms will be ignored for the moment. Let us consider a group

Table 1. Our calculated hfs components for the resonance Ag I and Au I lines.  $F_l$  and  $F_u$  represent the total momentum quantum numbers ( $F = J + I$ ) for lower (l) and upper (u) states of transition.  $\Delta\lambda$  (in pm) is a distance between the hfs component and its hfs-free wavelength.  $I_r$  represents relative intensities of the hfs components. The necessary atomic data are taken from [30].

Ag I 338.2889 nm			Ag I 328.0679 nm			Au I 267.5937 nm			Au I 242.7944 nm		
$F_l - F_u$	$\Delta\lambda$	$I_r$									
1-0	-0.18	50	1-1	-0.16	20	1-2	-0.96	100	1-0	-0.77	14.3
1-1	-0.16	100	1-2	-0.15	100	1-1	-0.91	20	1-1	-0.77	35.7
0-1	0.50	50	0-1	0.45	40	2-2	0.55	100	1-2	-0.77	35.7
						2-1	0.59	100	2-1	0.46	7.1
									2-2	0.46	35.7
									2-3	0.46	100

of atoms emitting light at a wavelength which corresponds to the same component present in the hfs pattern. Due to the intensive chaotic motion this component will appear as a broadened line. Under the assumption that the velocity distribution of the emitters is given by the Maxwell function, the line profile will be of the Gaussian type with corresponding half width. Repeating this consideration we will find that each hfs component is broadened by the Doppler effect, giving a line of the same halfwidth due to the fact that the emitters are essentially the same atoms with the same mass and velocity distribution. Consequently, the intensity of the light coming to the entrance slit of the spectrograph will be a superposition of the light intensities of individual hfs components. Therefore, at a given temperature  $T$  we have associated the same Gaussian parameter to all hfs components determined by the Doppler broadening [7]. The calculated resulting 267.595 nm Au I line shapes, at various plasma temperatures, are presented in Figure 6. Data for the hfs components separation (1.55 pm) and relative intensities (5 : 3, for the two groups of the components) are taken from Table 1. It is obvious that at high  $T$  all hfs details are lost due to the Doppler effect, and that equivalent distribution can be represented with a single Gaussian distribution with sufficient accuracy. However, at lower temperatures the components in the hfs begin to play an important role in the line shape formation. The same behavior shows the 242.795 nm Au I resonance line. It should be pointed out that the resonance Au I line shape characteristics give the possibility for diagnostics of a plasma with small  $B$  and  $N$  values.

It is quite difficult to say what is going on with the underlying structure of electron energy levels associated to the hfs in the strong electric fields present in high density plasmas. However, due to Doppler broadening at the temperatures reported here, all details

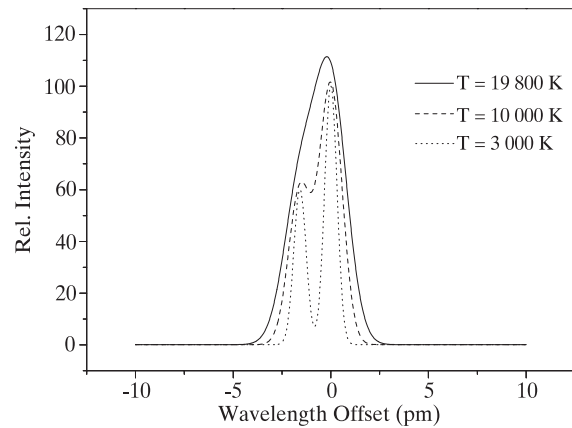


Fig. 6. Light intensity distribution obtained by superposition of 267.595 nm Au I line hfs components (see Table 1) broadened by Doppler effect for 3,000 K, 10,000 K and 19,800 K. Relative intensity on the y-axis follows from relative intensities of the hfs components (5 : 3). On the x-axis is the wavelength offset from the intense hfs component given in Table 1.

related to the splitting in the hyperfine structure are washed out. Therefore it is impossible to monitor the Stark effect of the particular hfs component. We can monitor only the behavior of the equivalent light intensity distribution caused by the Doppler broadening. In what follows our Stark width is associated to this 'averaged' spectral line.

Therefore, the Ag I and Au I line profiles represent the convolutions of the Lorentzian Stark (electron + ion) and Gaussian profiles caused by Doppler and instrumental broadening. For the electron density, electron temperature and density of the emitters in our experiment, the Van der Waals and resonance broadenings [7] were estimated to be smaller by more than one order of magnitude in comparison to the Stark, Doppler and instrumental broadening. We expect that the Ag II and Au II ion contributions to the total Stark

Table 2. Our measured Stark FWHM ( $W_m$  in pm) and shifts ( $d_m$  in pm) at a given electron density ( $N$  in units of  $10^{23} \text{ m}^{-3}$ ) and electron temperature ( $T$  in units of  $10^3 \text{ K}$ ) with the estimated accuracies ( $\pm 32\%$  for Au I and  $\pm 25\%$  for Ag I,  $\pm 0.8 \text{ pm}$ ,  $\pm 9\%$  and  $\pm 13\%$ , respectively). The hfs-free wavelengths are taken from [13]. Transitions are taken from [30]. Positive shift is shown toward red.  $W_{Th}$  and  $d_{Th}$  denote the sum of the calculated electron and helium ion contributions to the Stark parameters. They are taken from [14] and [15] for the Ag I and Au I lines, respectively (see also Figs. 7 and 8).  $W_D$  (in pm) denotes the estimated Doppler width calculated at a given electron temperature.  $\Delta_{hfs}$  (in pm) represents our calculated splitting in the hyperfine structure, while \* and \*\* denote these values obtained in [10] for Ag I, and in [11, 12] for Au I lines, respectively.

Emitter	Transition	$\lambda$ (nm)	$N$	$T$	$W_m$	$W_D$	$\Delta_{hfs}$	$d_m$	$\frac{W_m}{W_{Th}}$	$\frac{d_m}{d_{Th}}$	$\Delta_{hfs}$
Ag I	$5s^2S_{1/2} - 5p^2P_{3/2}^o$	328.068	$1.24 \pm 0.11$	$19.8 \pm 2.6$	$10.2 \pm 2.6$	3.19	0.61	$5.9 \pm 0.8$	1.10	1.44	$0.60^*$
	$5s^2S_{1/2} - 5p^2P_{1/2}^o$	338.289	$1.24 \pm 0.11$	$19.8 \pm 2.6$	$13.6 \pm 3.4$	3.29	0.68	$6.8 \pm 0.8$	1.50	2.06	$0.63^*$
Au I	$6s^2S_{1/2} - 6p^2P_{3/2}^o$	242.795	$0.78 \pm 0.07$	$16.8 \pm 2.2$	$8.0 \pm 2.6$	1.61	1.23	$2.2 \pm 0.8$	3.10	1.74	$1.28^{**}$
	$6s^2S_{1/2} - 6p^2P_{1/2}^o$	267.595	$0.78 \pm 0.07$	$16.8 \pm 2.2$	$9.8 \pm 3.1$	1.78	1.55	$3.0 \pm 0.8$	4.55	4.62	$1.58^{**}$

width is small (within 5%) and can be neglected, giving symmetrical line profiles. Therefore we have used the Voigt profile to fit our experimental Ag I and Au I line profiles (see the fitted Voigt profile in Fig. 2). This approximation results in slightly lower accuracies of the measured Stark width values.

For estimation of spectral line widths a deconvolution procedure [24], based on the least-squares algorithm, is applied. At each wavelength step we have recorded seven shots and, therefore, seven  $y$ 's are available to calculate the mean value and to estimate the interval of data scatter. Having scattered intervals, we applied a standard Monte-Carlo simulation (see [25], Section 14.5) to estimate the uncertainties of the best fit parameters. Using the foregoing procedure, we have associated uncertainties of  $\pm 32\%$  for Au I and  $\pm 25\%$  for Ag I Stark widths. The contribution of instrumental profile uncertainty is negligible. Estimation of the spectrum base line is done by applying the recently proposed method [23], which essentially measures the density of data points around a model function. The method is based on a new form of merit function (non-least-squares approach), which is insensitive for outlying points. In case of the spectrum presented in Fig. 2, an adequate model function is the straight horizontal line  $y = b$ . It implies that data points belonging to the spectral lines will be treated as outlying without any influence on the estimated magnitude of the base line.

The Stark shifts were measured relative to the unshifted spectral lines emitted by the same plasma. Thus, the Stark shift of a spectral line is measured by evaluating the position of the spectral line center recorded at different electron densities during the plasma decay (see [26] and references therein). The Stark shift was obtained with  $\pm 0.8 \text{ pm}$  accuracy [21].

#### 4. Results and Discussion

Our measured Stark widths ( $W_m$ ) and shifts ( $d_m$ ) of the Ag I and Au I lines are given in Table 2, together with the  $\Delta_{hfs}$  values and estimated Doppler widths ( $W_D$ ). In order to compare the measured and calculated Ag I and Au I Stark FWHM and shifts, we present in Figs. 7 and 8 the existing theoretical  $W$  and  $d$  data together with our new experimental values. Also, we have calculated the positions of the hfs components of the Ag I and Au I resonance lines from the known hf splitting constant [27]. Their relative intensities ( $I_r$ ) are calculated according to an analogy with  $LS$  coupling, as it is described in [27, 28]. The magnetic dipole interaction describing the coefficients ( $A$ ) are taken from [29] for the Ag I levels ( $A_{P_{3/2}} = -0.51 \cdot 10^{-3} \text{ cm}^{-1}$ ,  $A_{P_{1/2}} = -2.54 \cdot 10^{-3} \text{ cm}^{-1}$  and  $A_{S_{1/2}} = -57 \cdot 10^{-3} \text{ cm}^{-1}$ ) and from [14] for the Au I levels ( $A_{P_{3/2}} = 0$ ,  $A_{P_{1/2}} = 3 \cdot 10^{-3} \text{ cm}^{-1}$  and  $A_{S_{1/2}} = 105 \cdot 10^{-3} \text{ cm}^{-1}$ ). The electric quadrupole moments are zero. The obtained Ag I and Au I hfs characteristics are presented in Table 1.

On the basis of the obtained Ag I  $\Delta\lambda$  and  $I_r$  values one can conclude that splitting of higher levels, in both resonance transitions is present but it is very small. We have found strong asymmetry between the red and blue components in both lines. Two of three components in both lines are mutually very close (because the splitting of higher level is small), and these components can be treated as single. The results of hfs for both stable isotopes are very similar. Splitting in  $^{109}\text{Ag}$  is slightly higher.

In the case of the Au I lines one can conclude that the splitting of higher level, in both resonance transitions, is by two orders of magnitude smaller than the splitting of the ground level. For the 242.795 nm Au I

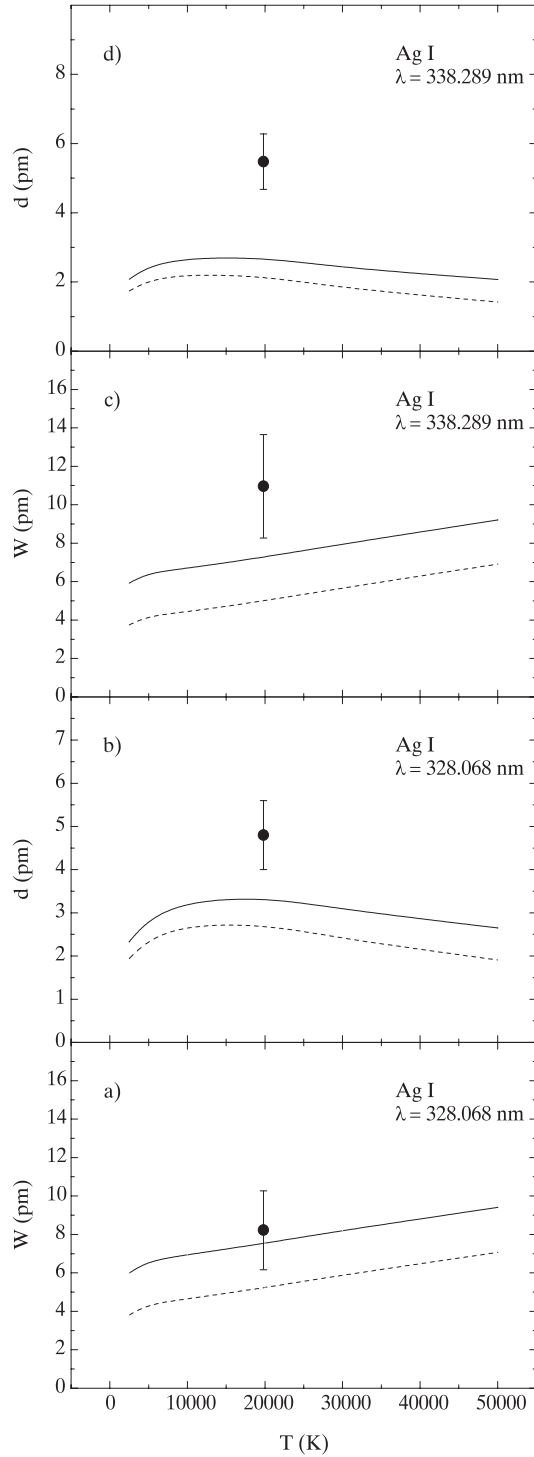


Fig. 7. Stark FWHM ( $W$ ) and shift ( $d$ ) dependences on the electron temperature ( $T$ ) at  $10^{23} \text{ m}^{-3}$  electron (and He II) density of the resonance Ag I lines. Dashed and solid lines denote theoretical values from [14] for electrons and electrons + helium ions as perturbers, respectively. Filled circles represent our measured values with their estimated accuracies.

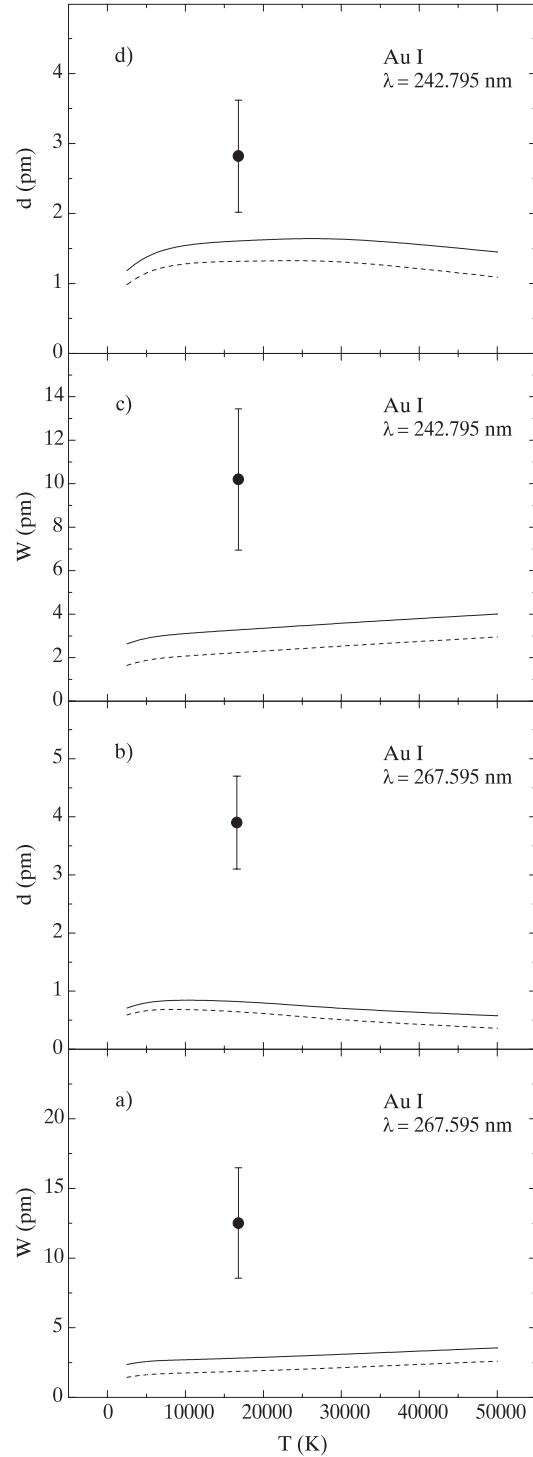


Fig. 8. Stark FWHM ( $W$ ) and shift ( $d$ ) dependences on the electron temperature ( $T$ ) at  $10^{23} \text{ m}^{-3}$  electron (and He II) density of the resonance Au I lines. Dashed and solid lines denote theoretical values from [15] for electrons and electrons + helium ions as perturbers, respectively. Filled circles represent our measured values with their estimated accuracies.

line the hyperfine splitting of the upper level can be neglected. For both lines the hfs components are clearly merged in two groups. Intensity ratio between groups is for both lines 5:3 if *LS* coupling is assumed as a good analogy for hfs.

We have found higher *W* and *d* values than the semi-classical approach provides. Namely, the mentioned works [14] and [15] refer on the small electron contribution ( $W_e$  and  $d_e$ ) to the resonance Ag I and Au I *W* and *d*. It should be mentioned that the calculated  $W_e$  values, at  $10^{23} \text{ m}^{-3}$  electron density, are of the same order as the splitting in the hfs (see Table 2 and Fig. 8) for the two Au I lines. Besides the electrons, the helium ions (He II) play also an important role in the Ag I and Au I lines broadening. The authors of [14] and [15] have predicted a He II contribution up to 50% of the electron contribution for both Stark parameters. We have compared our  $W_m$  and  $d_m$  values with the sum of the electron and helium ion contributions ( $W_{Th}$  and  $d_{Th}$ ). The ratios  $W_m/W_{Th}$  and  $d_m/d_{Th}$  are included in Table 2. Agreement with the calculated values was found in the case of the 328.068 nm Ag I line. Extreme disagreement (up to 4.6 times) was found in the case of the 267.595 nm Au I line. At our plasma conditions the  $\Delta_{hfs}$  are overpowered by Stark broadening for resonance Ag I and Au I lines. Moreover, in the case of the Ag I lines the Doppler width (see  $W_D$  in Table 2) is also higher than  $\Delta_{hfs}$ . Because the *W* and  $W_D$  values are proportional to *N* (approximately) and  $\sqrt{T}$ , respectively, we can estimate the plasma parameters that give a single line broadening smaller than  $\Delta_{hfs}$ . In the case of the 267.595 nm Au I line they are  $T \leq 10,000 \text{ K}$  and  $N \leq 10^{20} \text{ m}^{-3}$ . Below these estimated plasma parameters the components in the hyperfine structure play an important role in the mentioned line shape formation. This is explicitly shown in Fig. 6 for temperatures below 10,000 K. So, the Au I 267.595 nm line shape characteristics can be used for temperature diagnostics in emission spectra of cold optically thin plasmas.

We have found positive Stark shifts. Theoretical predictions are also positive (see Figs. 7 and 8). Our  $d_m$  values are about 8.5 and 2.3 times higher than the related  $\Delta_{hfs}$  values in the case of the Ag I and Au I lines, respectively, at  $10^{23} \text{ m}^{-3}$  electron density. The authors in [15] have calculated Au I line electron Stark shifts at  $10^{23} \text{ m}^{-3}$  electron density that lie inside the  $\Delta_{hfs}$  values (see Table 2 and Fig. 8).

## 5. Conclusion

The shapes and shifts of the neutral silver and gold resonance spectral lines have been obtained in a laboratory helium plasma at about 18,500 K electron temperature and electron density ranging between  $0.78 \cdot 10^{23}$  and  $1.24 \cdot 10^{23} \text{ m}^{-3}$ . Our measured Ag I and Au I resonance line Stark widths and shifts are the first reliable experimental data. They are higher than the calculated ones, especially in the case of the Au I resonance lines. It has been found that at the mentioned plasma conditions the Stark broadening is the dominant mechanism of the line shape and position formation. At the above mentioned helium plasma conditions the splitting in the hyperfine structure of the Ag I and Au I resonance lines has been overpowered by Stark and Doppler broadenings. We estimate that at electron densities below  $10^{20} \text{ m}^{-3}$  and electron temperatures below 10,000 K the hfs components in the 267.595 nm and 242.795 nm Au I lines play an important role in the line shape formation, and the resulting line profiles can be used for temperature estimation in optically thin plasmas.

## Acknowledgements

This work is part of the projects "Determination of atomic parameters on the basis of spectral line profiles" and "Stellar and solar physics" supported by the Ministry of Science and Environmental Protection of the Republic of Serbia. The authors are thankful to the corporation "Zlatara Majdanpek" for providing gold plates.

- [1] S. J. Adelman, C. R. Proffitt, G. M. Wahlgren, D. S. Leckrone, and L. Dolk, *Astrophys. J. Supp. Ser.* **155**, 179 (2004).
- [2] C. Sneden, J. J. Cowan, J. E. Lawler, I. I. Ivans, S. Burles, T. C. Beers, F. Primas, V. Hill, J. W. Truran, G. M. Fuller, B. Pfeiffer, and K.-L. Kratz, *Astrophys. J.* **591**, 936 (2003).
- [3] G. M. Wahlgren, L. Dolk, G. Kalus, S. Johansson, U. Litzén, and D. S. Leckrone, *Astrophys. J.* **539**, 908 (2000).
- [4] S. Xu and R. E. Sturgeon, *Spectrochim. Acta B* **60**, 101 (2005).
- [5] A. Hamel, A. Schier, and H. Schmidbaur, *Z. Naturforsch.* **57b**, 877 (2002).
- [6] H. R. Griem, *Plasma Spectroscopy*, McGraw Hill, New York 1964.

- [7] H.R. Griem, *Spectral Line Broadening by Plasmas*, Academic Press, New York 1974.
- [8] C. Schwartz, *Phys. Rev.* **97**, 380 (1955).
- [9] G.H. Fuller and V.W. Cohen, *Nucl. Data Tables A* **5**, 433 (1969).
- [10] H. Hill, *Phys. Rev.* **48**, 233 (1935).
- [11] R. Ritschl, *Naturwissenschaften* **19**, 690 (1931).
- [12] R.M. Elliott and J. Wulff, *Phys. Rev.* **55**, 170 (1939).
- [13] NIST – Atomic Spectra Data Base Lines, <http://physics.nist.gov> (2006).
- [14] M.S. Dimitrijević and S. Sahal-Bréchet, *At. Data Nucl. Data Tables* **85**, 269 (2003).
- [15] L.Č. Popović, M.S. Dimitrijević, and D. Tankosić, *A&AS* **139**, 617 (1999).
- [16] S. Djeniže, A. Srečković, J. Labat, R. Konjević, and L. Popović, *Phys. Rev. A* **44**, 410 (1991).
- [17] S. Djeniže, A. Srečković, and S. Bukvić, *Spectrochim. Acta B* **60**, 1552 (2005).
- [18] S. Djeniže and S. Bukvić, *A&A* **365**, 252 (2001).
- [19] S. Djeniže, A. Srečković, and S. Bukvić, *Z. Naturforsch.* **60a**, 282 (2005).
- [20] S. Djeniže, A. Srečković, and S. Bukvić, *Z. Naturforsch.* **61a**, 91 (2006).
- [21] S. Bukvić, A. Srečković, and S. Djeniže, *New Astron. A* **9**, 624 (2004).
- [22] A. Srečković, S. Bukvić, and S. Djeniže, *Phys. Scr.* **72**, 18 (2005).
- [23] S. Bukvić and D. Spasojević, *Spectrochim. Acta B* **60**, 1308 (2005).
- [24] J. T. Davies and J. M. Vaughan, *Astrophys. J.* **137**, 1302 (1963).
- [25] H. W. Press, B. P. Flannery, S. A. Teukolsky, and W. T. Vetterling, *Numerical Recipes*, Cambridge University Press, Cambridge 1988.
- [26] S. Bukvić, A. Srečković, and S. Djeniže, *Z. Naturforsch.* **59a**, 791 (2004).
- [27] E.U. Condon and G.H. Shortley, *The Theory of Atomic Spectra*, Cambridge University Press, Cambridge 1964.
- [28] N. Vitas, MSc Thesis, Faculty of Mathematics, Belgrade 2005 (unpub.).
- [29] J. Carlsson, A. Dönszelman, H. Lundberg, A. Persson, L. Sturesson, and S. Svanberg, *Z. Phys. D* **6**, 125 (1987).
- [30] R.L. Kurucz, *Atomic Spectral Line Database from CD-ROM* 23.